Author Version of : Environmental Research Letters, vol.16(1); 2020; Article no: 14027

Increased cyclone destruction potential in the Southern Indian Ocean

Vidya P. J[1]*, Ravichandran M[1], R. Murtugudde[2,3] , Subeesh M. P[1], Sourav Chatterjee [1], Neetu S[4], Nuncio M[1]

[1]National Centre for Polar and Ocean Research (NCPOR), Ministry of earth sciences, Headland Sada, Goa - 403 804, India.

[2]Interdisciplinary Programme in Climate Studies, Indian Institute of Technology, Bombay, India, ESSIC.

[3]University of Maryland, College Park, MD, USA.

[4]CSIR-National Institute of Oceanography, Dona Paula, Goa 403004, India

*Corresponding author email: vidya@ncpor.res.in

Abstract

The present study examines the role of the Southen Indian Ocean (SIO) warming on the cyclone destruction potential or power dissipation Index (PDI) during two contrasting periods of 1980-1998 and 1999-2016. The PDI in the SIO during 1999-2016 is found to have doubled compared to the same during 1980-1998. PDI was computed using the tropical cyclone track data in the SIO region for cyclone category three and above. The increasing trend in PDI during the latter period is primarily due to an increase in the intensity of cyclones and their duration. The increasing PDI is associated with a sea surface temperature warming and an upper ocean heat content increase as well as a significant slowdown in translation speeds. The increase in upper ocean heat content during the recent decades enhances the intensification of cyclones and their duration, which is consistent with the slowdown of cyclones. Analysis of the relevant atmospheric parameters indicates that processes in the atmosphere did not play a major role in the recent decades in increasing cyclone intensity. We show that in the SIO, ocean processes play a major role in the PDI rise during the recent period. Any continued increase in PDI will cause more loss of life and socioeconomic damage to the island countries such as Mozambique, Mauritius, Mascarene Islands and Madagascar, as well as the coastal inhabitants along East Africa.

Keywords: Southern Indian Ocean, Power dissipation Index, Tropical Cyclones, Slowdown of Cyclones, Sea surface temperature.

Key points:

- Increased cyclone power dissipation index (PDI) occurs in the southern Indian Ocean during 1999-2016.
- Increase in PDI during the recent two decades is contributed by warmer sea surface temperatures and increased upper ocean heat content.

1. Introduction

Tropical cyclones (cyclones in the Indian Ocean), also called typhoons (in the Pacific) or hurricanes (in the Atlantic), are among the most hazardous natural calamities that affect the coastal regions (Blake *et al* 2011). Tropical cyclones (TCs hereafter) are characterized by intense circular storm centered around low atmospheric pressure, with strong winds, and heavy rainfall causing loss of life and property damage. Variability and change in the number, intensity and rate of intensification of the TCs are vital owing to their observed response to global warming (Li *et al* 2010). On the positive side, TCs contribute significantly to rainfall over the affected regions (Lyon & Camargo, 2009; Pezza et al., 2012). Cyclones are argued to be a part of the poleward heat transport required by the equator-to-pole temperature gradient (Emanuel 2001, Uotila *et al* 2011). Due to its atmospheric and oceanic properties, a large number of tropical cyclones form in the Southwestern Indian Ocean, which also show a relation to the modes of coupled climate variability (Burns *et al* 2016).

The loss of property and life have been well-documented in this region. For example, tropical cyclone 'Idai' (4 - 21 March 2019) was one of the most severe tropical cyclones that affected the southern Indian Ocean. Idai made landfall in Mozambique, where more than 1300 people were killed, and more than 3 million people were directly affected. It is one of the costliest cyclones in the southwestern Indian Ocean, with total damage estimated at approximately $2.2 billion. Just after four weeks of cyclone Idai, another intense cyclone 'Kenneth' formed in the region during 21-29th April 2019, which also caused considerable socioeconomic damage. With the expected continuation of the Indian Ocean warming, and its relation and feedback to the Pacific warming, the importance of understanding the factors influencing the number and intensity of TCs in this region is obvious (Zhang *et al* 2019b).

Earlier studies (Emanuel, 2005; Webster, 2005) have shown that cyclone frequency, and intensity are directly linked to an increase in sea surface temperatures (SST) caused by natural modes of climate variability and/or global warming. Vidya *et al.,* (2020) and Zhang *et al.*, (2018) have reported that the Southern Indian Ocean (SIO) SST and upper ocean heat content have increased significantly during the last two decades. This warming is mainly due to the increased advection of upper-ocean warm water from the western Pacific through the Indonesian Throughflow (ITF; Dong and McPhaden 2016; Lee et al., 2015; Zhang et al., 2018). The apparent secular variability in the tropical Pacific warming continues to be debated (England *et al* 2014), especially in terms of the relative warming rates of the eastern and western halves of this important region (Cane *et al* 1997,

Kosaka and Xie 2013a, England *et al* 2014, Zhang *et al* 2018, Seager *et al* 2019). Increased advection of this warm western Pacific water into the SIO (Vidya et al., 2020) can significantly contribute to the TC characteristics in this region. Warmer oceanic regions can support the enhanced intensification of the cyclones by supplying more energy from the upper ocean (Emanuel, 2000; Wing et al., 2007). However, our aim is not to engage in a debate about the global warming responses of the Pacific and Indian Oceans or the relation between them, since the role of the Southern Ocean warming in the Indian Ocean warming may also be an important consideration which has not received as much attention (Jayasankar *et al* 2019b). Our main goal in this study is to examine the role of SIO warming on the cyclone destruction potential or power dissipation Index (PDI) during two contrasting periods of 1980-1998 and 1999-2016. The choice of the dividing year for the two periods is motivated more by the proposed regime shift (Swanson and Tsonis 2009) which has also served as the debating point for the so-called global warming hiatus. This is discussed further in the Data and Method section below.

2. Data and Method

Most of the cyclones (~85 %) in the SIO occur from November to April (Mavume *et al* 2010). Hence, all the analyses in this study are performed for the period November-April and referred to as the 'cyclone season'. The PDI, a commonly used parameter to depict the destructive potential of tropical cyclones, is defined as the cube of the 6-hourly maximum surface wind speed integrated over the lifespan of the cyclones (Emanuel, 2005). The PDI is computed using the methodology provided by Emanuel, (2007) as follows,

$$PDI = \int_0^{\tau} V_{max}^3 \, dt \qquad (1)$$

Where V_{max} is the maximum surface wind speed at each 6-hourly time interval (t) over the cyclone duration (τ). The annual PDI in each year is defined as the summation of all the cyclones (N) that occur during the cyclone season (November-April). In order to avoid the over-weighting of the contribution by any particular cyclone, Emanuel, (2007) proposed velocity-weighted duration (D_{wt_i}) of a cyclone as follows,

$$D_{wt_i} = \frac{\int_0^{\tau} V_{max} dt}{V_{smax}} \qquad (2)$$

Where V_{smax} is the lifetime peak intensity of the cyclone. The average duration of all the cyclones in each season is calculated as follows,

$$D_{wt} = \frac{1}{N} \sum_1^N D_{wt_i} \qquad (3)$$

The annual averaged intensity (in wind speed cubed) during November-April in each year is calculated as follows,

$$I = \frac{\sum_1^N \int_0^{\tau_i} V_{max}^3 dt}{\sum_1^N D_{wt_i}} \quad (4)$$

The above parameters are calculated using the best-track tropical cyclone data obtained from the Joint Typhoon Warning Center (JTWC; source: https://www.metoc.navy.mil/jtwc/jtwc.html?southern-hemisphere). The JTWC maintains an archive of tropical cyclone data, known as "best tracks" and each best-track data contains positions of tropical cyclone locations and intensities (maximum sustained surface winds) at every six-hourly interval. We use the Saffir-Simpson scale to define tropical cyclone categories. As per Saffir-Simpson scale, wind speeds ranging from 17-33 m s^{-1} are defined as a tropical storm (Cat-0), 33 - 43 m s^{-1} as category-1 (Cat-1), 43-50 m s^{-1} as category-2 (Cat-2), 50-59 m s^{-1} as Category 3 (Cat-3), 59-70 m s^{-1} as category 4 (Cat-4) and greater than 70 m s^{-1} as category 5 (Cat-5) tropical cyclones. Cyclones of category 3 and above tend to cause more catastrophic devastation over land. In addition, major oceanic and atmospheric responses occur only when the cyclone winds become stronger than 59 m s^{-1} (category 3). Hence, in the present study, we have considered only TCs with the intensity level of category 3 and above. Our conclusions on the trends are not altered by considering all the categories.

Since a cyclone can impact far away regions from its center, all the atmospheric variables are averaged over the region within a 1000 km radius from the center of the cyclone track during the days of the cyclone passage. Atmospheric variables such as relative humidity at 600 hPa, winds at 850 hPa and 200 hPa, geopotential height at 850 hPa and the mean sea level pressure for the period 1980 to 2016 are obtained from daily means of ERA-interim (Dee *et al* 2011) with a spatial resolution of 0.75 degree x 0.75 degree. Winds at 850 hPa are used to calculate relative vorticity. Vertical wind shear is calculated based on the wind speed difference between 200 hPa and 850 hPa using the following equation:

$$Vertical\ Wind\ Shear\ (VWS) = \sqrt{(U_{200hPa} - U_{850hPa})^2 + (V_{200hPa} - V_{850hPa})^2} \quad (5)$$

With the above, the annual mean of each parameter (relative vorticity, relative humidity, and vertical wind shear) for each year is calculated.

Monthly mean sea surface temperature is obtained from the Met Office Hadley Centre's sea ice and sea surface temperature dataset (HadlSST1) for the period 1980 to 2016 (Rayner *et al* 2003)

with a spatial resolution of 1 degree x 1 degree. The upper-ocean heat content *(UOHC)* in the upper 200 m is calculated using the equation

$$UOHC = \rho_o C_p \int_0^h T(z)\ dz \qquad (6)$$

Where ρ_o is the reference density of seawater (1027 kg m^{-3}), C_p is the heat capacity of the sea water at constant pressure, h is the deepest layer of integration (200 m here), and T is the potential temperature. The monthly mean ocean potential temperature with a spatial resolution of 1 degree x 1 degree is acquired from the European Centre for Medium-Range Weather Forecasts (ECMWF) Ocean Reanalysis System 4 (ORAS4) (Balmaseda *et al* 2013). The least-squares linear regression test has been performed to evaluate the trends. Significance of all the trends are tested with two-tailed t-test at 95% confidence interval. Details of the statistical analysis are given in Table 1.

In the present study, we have considered the cyclone characteristics in the SIO for two periods; 1980-1998 and 1999-2016. As mentioned in the Introduction, a regime shift in climate was proposed around 1999 by Swanson and Tsonis (2009), but a debate has also raged about a potential slowdown in global warming as also stated in the Introduction (Kosaka and Xie 2013b, England *et al* 2014, Zhang *et al* 2018). Since the cyclone season in the SIO extends from November of one year to April of the following year, in the present study, we have considered the year starting from 1999 as the dividing line. As an aside, we note that some earlier studies (for example, Zhang *et al* 2019a, Hu and Fedorov 2017) have argued that weakening of global warming trend ceased in 2012 and a strong warming occurred during the period 2014-2016; these three years are the three warmest years for our study period. However, SIO shows a similar warming trend starting from 1998 to the end of 2016 (Vidya et al., 2020). Re-emphasising that our goal is not to focus on the so-called Global Warming Hiatus, we just contrast the two periods for the cyclone characteristics and their putative driving mechanisms during the two periods.

3. Results and Discussion

The PDI in the SIO region (5^{o}S-25^{o}S and 40^{o}E-100^{o}E) shows ~100% increase during the recent decades (1999-2016) compared to the preceding two decades (1980-1998) (Figure 1a), i.e., almost a doubling. Although the trends are positive during both the periods, the trend was not significant during the first period. The PDI was computed using the tropical cyclone trajectories shown in Figure 1b and 1c, respectively. Note that an apparent westward shift in the average position of the cyclogenesis location is evident during the second period. The interannual variability is also much higher during the latter period compared to the first period, the reasons for which are not the focus here.

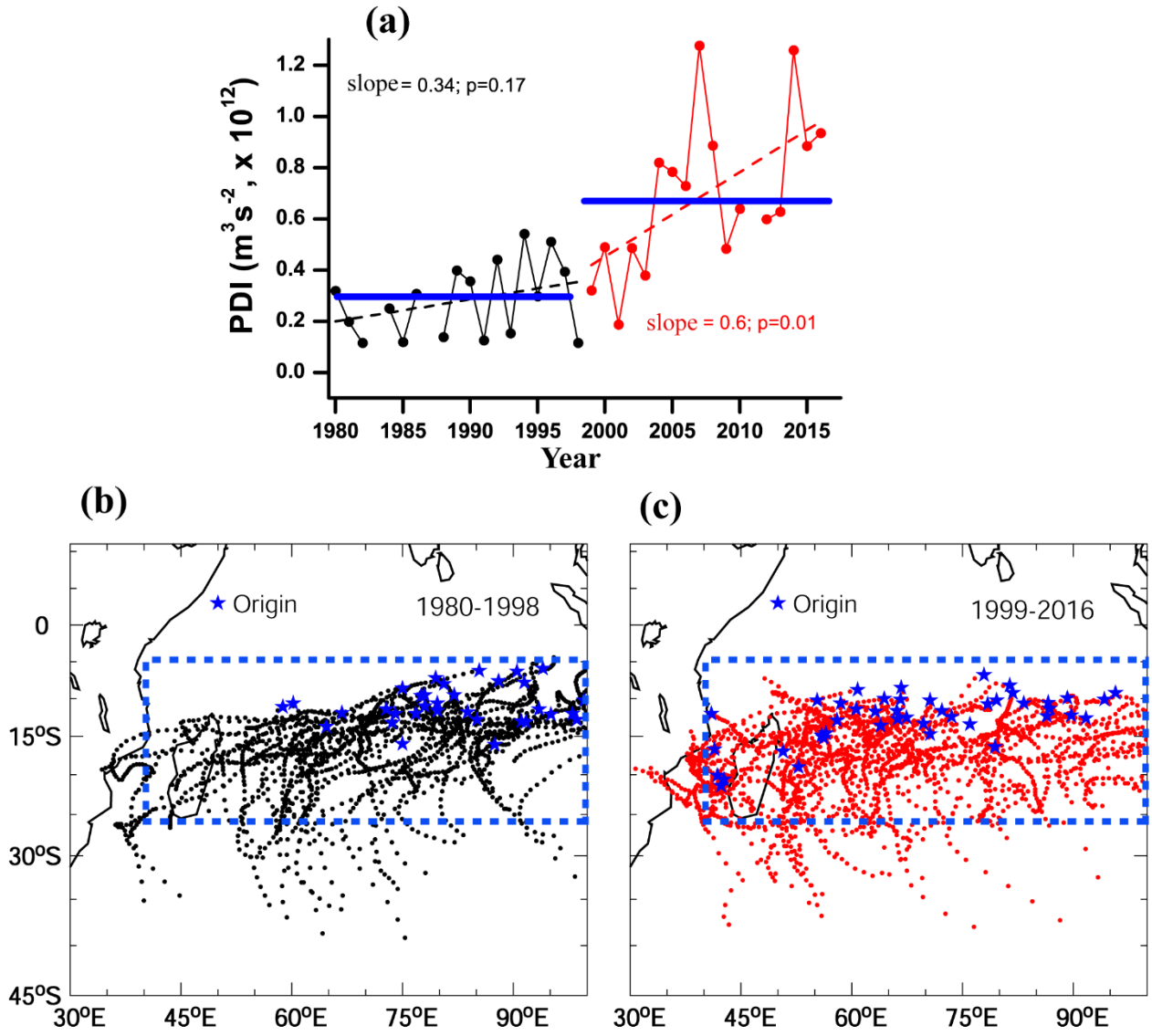

Figure 1: (a) Time series of the Power dissipation Index (PDI); horizontal blue lines indicate the mean PDI for the respective period. Cyclone tracks (category three and above) (b) during 1980-1998 and (c) during 1999-2016, in the southern Indian Ocean. Blue stars indicate the cyclone origins and the blue dashed box indicates the cyclogenesis (40°E-100°E and 5°S-25°S) region. In (a), slope indicates the regression value and 'p' values indicate the significance of the trends. The missing years in (a) indicate the absence of cyclones with category 3 and above.

To understand the reason for the increase (doubling) in PDI during the recent period, we examined three important factors, viz., cyclone intensity (I), duration (D), and frequency (N) which control the PDI. Duration is the average lifespan of a cyclone calculated based on velocity-weighted duration following equations (2) and (3). Here, we assessed the individual variables to understand the importance of each component to the PDI during both the periods. Similar to PDI (Figure 1a), the intensity of cyclones also showed an increasing trend in both the periods, with a stronger trend during 1999-2016 (Figure 2a). A significant increasing trend in the duration (Figure 2b) and a

decreasing trend in the number of cyclones (Figure 2c) is observed during the recent decades. However, neither the duration nor the number of cyclones show any significant trend during the first period (Figure 2b & 2c). Note again that the cyclone PDI, the intensity and duration increased significantly during 1999-2016 compared to 1980-1998 (Table 1).

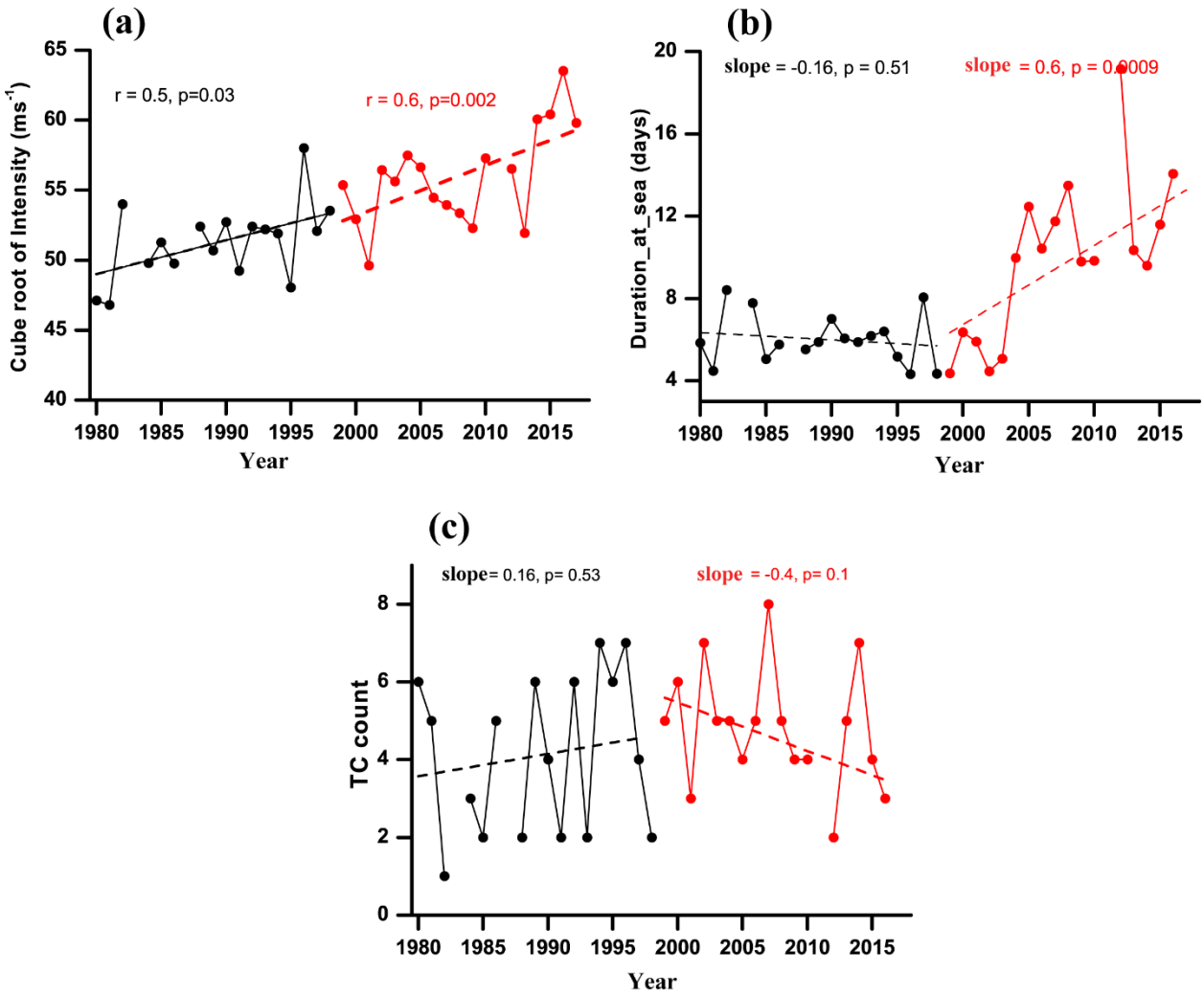

Figure 2: Time series of factors contributing to PDI. (a) Averaged intensity in m/s (cube root of Intensity), (b) averaged cyclone duration in days, and (c) cyclone count in the SIO during the cyclone season (Nov-Apr). The black line indicates the first period and red line the second period. Slopes indicate the regression value and 'p' values indicate the significance of trends. Missing years correspond to the absence of cyclones of category 3 and above.

Malan et al. (2013) showed that in the SIO, a stronger anticyclonic condition to the east of Madagascar causes a decreasing trend in tropical cyclones after the monstrous 1997-98 El Niño event. Girishkumar & Ravichandran (2012) showed that in the Bay of Bengal, positive SST

anomalies during El Niño events cause atmospheric changes which result in a reduction in the number of cyclones. Consistent with the above studies, we also observe a strengthening anticyclonic pattern to the east of Madagascar during recent decades (Figure S1). Based on Figures 2a and b, it can be argued that during 1999-2016, the increasing trend in PDI is due to positive trends in the intensity of the cyclones and their duration. To elicit the reasons for the increase in cyclone intensity and duration from the first to the second period, we further explore the oceanic and atmospheric factors that can influence them.

3.1 Oceanic parameters and cyclone Intensity

Figures 3a and 3b depict the annual mean SST and upper ocean heat content (UOHC) in the cyclogenesis region (40^{o}E-100^{o}E; 5^{o}S-25^{o}S). SST and UOHC are the important oceanic parameters which are directly linked to the cyclone intensity, and hence the PDI (Emanuel et al., 2004; Lin et al., 2008, 2013). SST (Figure 3a) and UOHC (Figure 3b) show an increasing trend during the latter period, while trends are not significant during the former. The mean UOHC in the cyclogenesis region has increased by ~0.45 x 10^{9} J m^{-2} during the second period compared to the first, and the difference is statistically significant (Table 1). In addition, we also calculated the annual mean translation speed during both the periods. The average translation speed during the first period was 4.3 ± 0.5 m s^{-1}, while during the second period it slowed down to 2.7 ± 0.8 m s^{-1}. In contrast to the SST and UOHC, cyclone translation speed showed a significant decreasing trend across the two periods (Figure 3c).

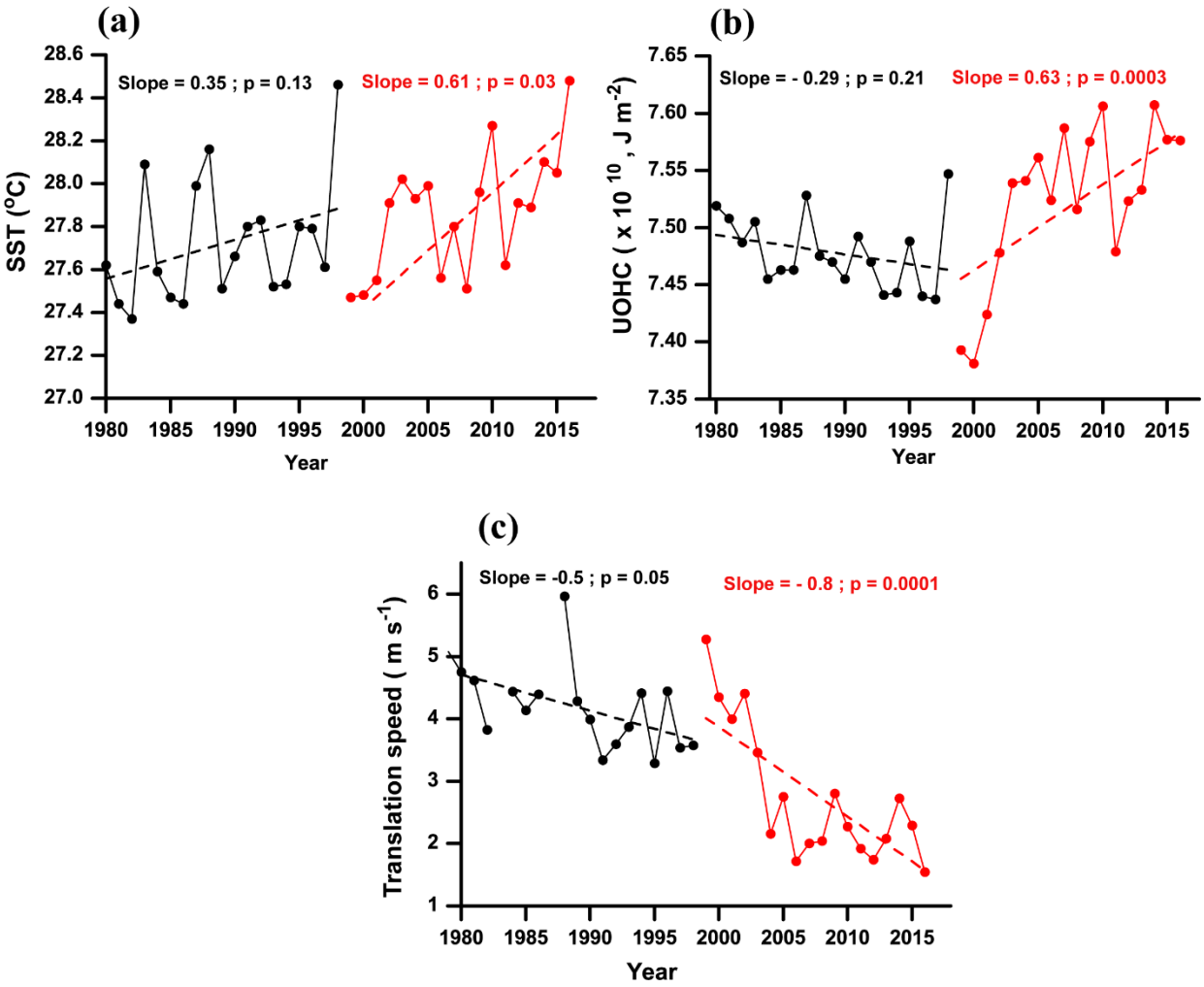

Figure 3. Time series of annual mean (a) SST and (b) Upper ocean heat content (UOHC) in the cyclogenesis region (40°E-100°E and 5°S-25°S) and (c) Cyclone translation speed calculated from the cyclone tracks. Black dotted lines indicate the trend during 1980-1998 and red dashed lines indicate the trend during 1999-2016. The slope indicates the regression value and 'p' values indicate the significance of the trends.

To identify the exact mechanism for the increase in PDI during the recent decades, we perform a spatial correlation analysis between UOHC and PDI (Figure 4a). The UOHC shows a significant positive correlation with the PDI in the cyclogenesis region (Figure 4a), indicating that PDI and UOHC are strongly related during the recent decades. In addition, the temporal correlation between UOHC and intensity is also positive ($r = 0.54$, $p = 0.03$; Figure 4b), implicating the increase in UOHC for increased intensification of cyclones and thus the increases in PDI. This is mainly because, the increase in SST and UOHC help to intensify the cyclone by the sustained supply of heat fluxes to the atmosphere (Emanuel 1987, Mawren and Reason, 2017). Our results are consistent with the previous studies (Manatsa, et al, 2012; Malan, et al, 2013; Dilmahamod, et al, 2016; Mawren and Reason, 2017), which also showed an increase in UOHC over the SIO for the post-1997

El Niño period. We further analyse how these increases in cyclone intensity affect the cyclone duration and translation speed.

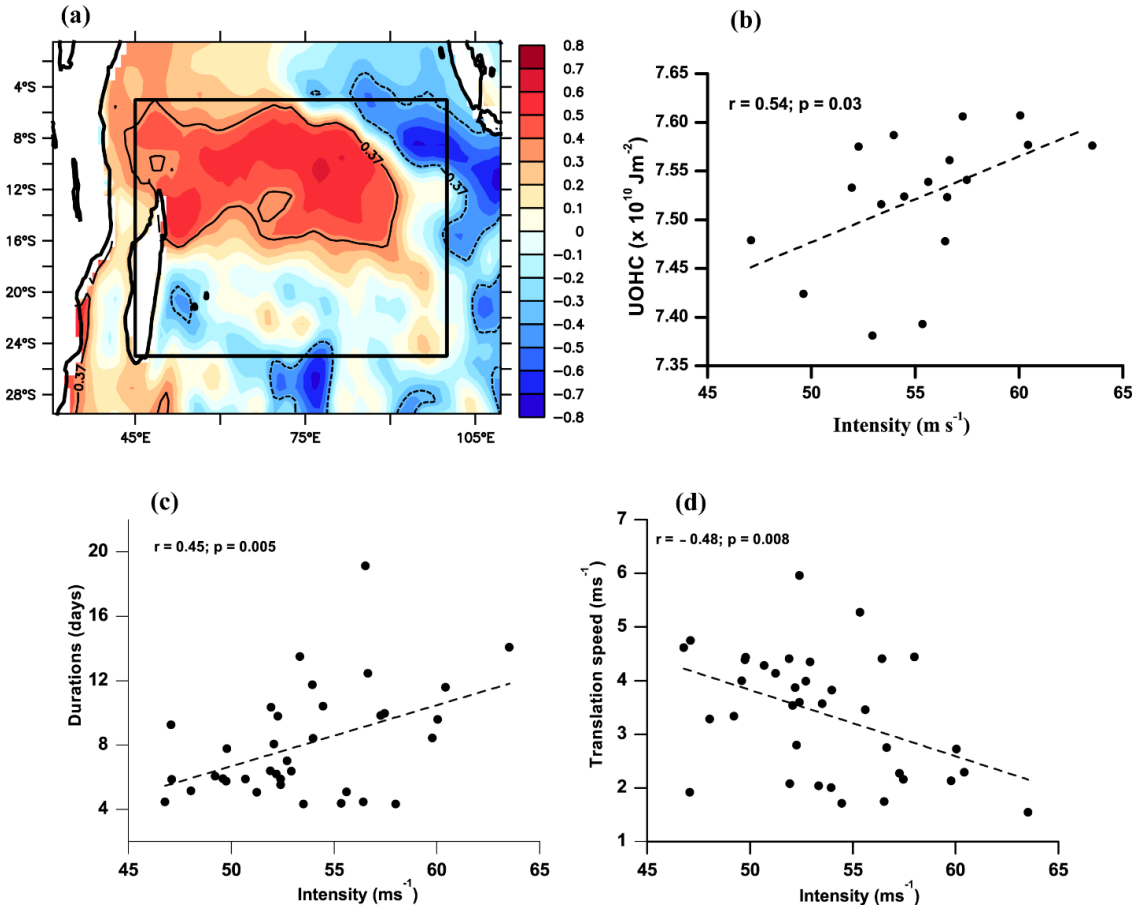

Figure 4: Spatial correlation between (a) PDI and UOHC during 1999-2016. Temporal correlation between, (b) Intensity vs. UOHC, (c) Intensity vs. duration, and (d) Intensity vs. translation speed. Black contours in Figure 4a indicate the 90 % confidence level.

Cyclone intensity vs. duration shows a positive correlation as well (r = 0.45; p = 0.005; Figure 4 c). However, intensity vs. translation speed shows a negative correlation (r = - 0.48; p = 0.008; Figure 4 d). This further confirms that the increase in intensity during the recent decades causes an increase in cyclone duration associated with a reduced translation speed. Thus the increased UOHC in the SIO can be blamed for the increased cyclone intensity and duration (Emanuel, 2015; Webster, 2005; Malan et al., 2013) due to a more persistent energy availability from the ocean to the surface during the life cycle of a cyclone (Mawren and Reason 2017). Bhatia *et al* (2019) report a recent increase in cyclone intensification rates in the Atlantic basin associated with the warming there and our results are consistent with their findings.

In addition, spatial maps of anomalies (second – first period) of SST (Figure 5a), thermocline depth (Figure 5b) and heat content in the upper 200 m (Figure 5c) also display positive changes to

the east of Madagascar reaffirming the significant warming of the upper ocean (SIO) across the decades. A deeper thermocline and a larger heat content in the western SIO during the latter period impede SST cooling during the cyclone passage and favour reduced cyclone translation speed and underlie its intensification into stronger categories.

The negative correlation between the cyclone intensity and translation speed (Figure 4 c) further supports our hypothesis. Hence, we believe that the increase in the intensity of the tropical cyclone in the SIO is primarily due to warming of the upper ocean even though we make no arguments for the processes that caused the warming itself. We do want to add a caveat that the upper-level steering winds are also argued to be important for the slowdown of the cyclones across the globe (Kossin 2018) which is not considered here.

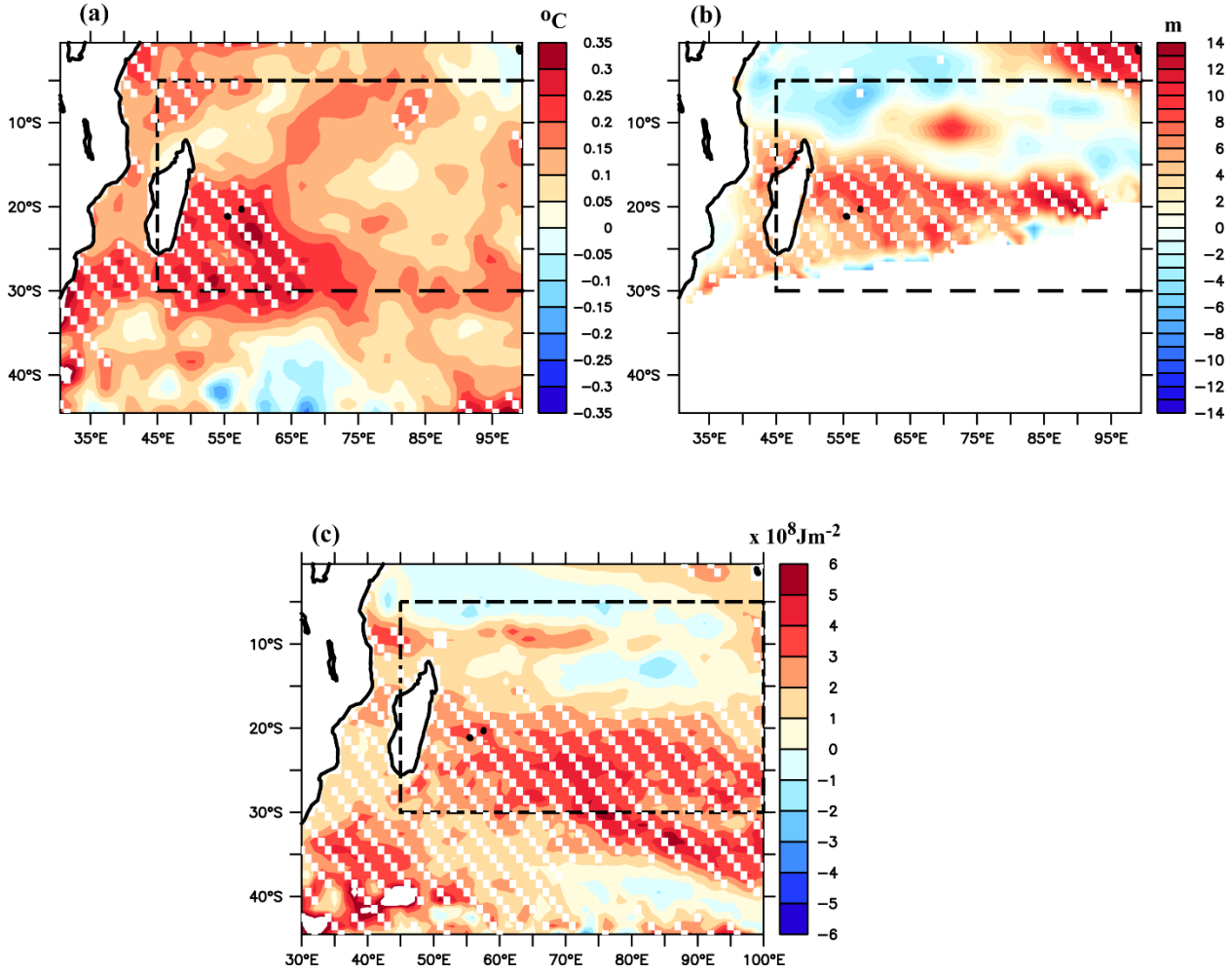

Figure 5: Differences between 1999-2016 and 1980-1998 in (a) sea surface temperatures between 1999-2016 and 1980-1998, (b) thermocline depth (D26), (c) upper ocean heat content. Black dashed rectangle indicates the cyclogenesis region. White dots represent anomalies above the 90% significance level.

Recent studies (Dong and McPhaden 2016; Liu *et al.*, 2015; Zhang *et al.*, 2018; Jyoti *et al.*, 2019; Vidya et al., 2020) have indicated a significant warming of the SIO since the end of the 20th century. Zhang et al. (2018) showed that an increased Indonesian Throughflow (ITF) during the recent decades is the major contributor to the warming in the upper 700m of the SIO. Intensification of the trade winds over the tropical Pacific during the recent decades has been argued to cause an increase in the ITF (Liu *et al* 2015, Hu and Sprintall 2017) and transport more heat from the western Pacific into SIO. Lee et al. (2015) showed that during the recent period, Pacific Ocean heat content decreased with a simultaneous increase in the SIO heat content. The abrupt increase (70% of the global ocean heat) in the SIO heat content and cooling (reduced heat content) in the tropical Pacific was also blamed on the ITF by Ueda *et al* (2015). The detailed mechanism of the SIO warming since 1998 and its implications are described in Vidya et al., (2020). More recently, Jyoti et al. (2019) have shown that the resultant warming of the SIO caused an increase in seal level rise which is 37% faster in the SIO than the global mean sea-level rise after the regime shift of 2000. Thus, warming of the SIO during the latter period of our study results in increasing trends in cyclone intensity and duration, which contribute to the total increase in PDI. As noted earlier, the Indian Ocean meridional overturning circulation can be expected to play a role in the tropical Indian Ocean warming as well, although the timescales of this direct link between the Southern Ocean and the tropical Indian Ocean remain to be quantified.

3.2 Influence of atmospheric variables on cyclone intensity

In addition to the oceanic parameters, we also assess the atmospheric contribution to the increased cyclone intensity and duration from the first to the second period. The vital atmospheric factors which can influence the cyclone intensity are (1) low-level relative vorticity at 850 hPa (Figure 6a), (2) high relative humidity (RH) at 600 hPa (Figure 6b), and (3) minimum vertical wind shear (VWS; Figure 6c) between 850 hPa and 200 hPa (Emanuel, 2005). All the atmospheric variables are taken within a 1000 km radius from the center of the cyclones (along their tracks) during the same days of the cyclone passage. Minimum VWS, maximum relative vorticity and relative humidity are the main atmospheric dynamic and thermodynamic factors necessary for the formation of a cyclone (Emanuel 2007, Matsuura *et al* 2003). During the first period, only the low level relative vorticity shows an increasing trend (slope = - 0.44; p = 0.08), whereas relative humidity (slope = 0.14; p = 0.57) and vertical wind shear (slope = -0.01; p = 0.96) show no significant trends. However, during the latter period, none of the atmospheric variables, i.e., relative vorticity (slope = -0.1; p= 0.45), relative humidity (slope = 0.023; p = 0.88) or vertical wind shear (slope = 0.07; p = 0.76), show any significant trend. To further substantiate this, we also examine variations in

atmospheric variables along the cyclone tracks during the two periods (Figures S2 and S3). It is apparent that no significant differences in atmospheric parameters along the cyclone tracks occur in either period. We can conclude from these that the atmospheric processes likely did not directly contribute to the increase in cyclone duration and intensity. This also underscores our assertion that the cyclone PDI has increased in the recent decades because of the increase in SST and heat content.

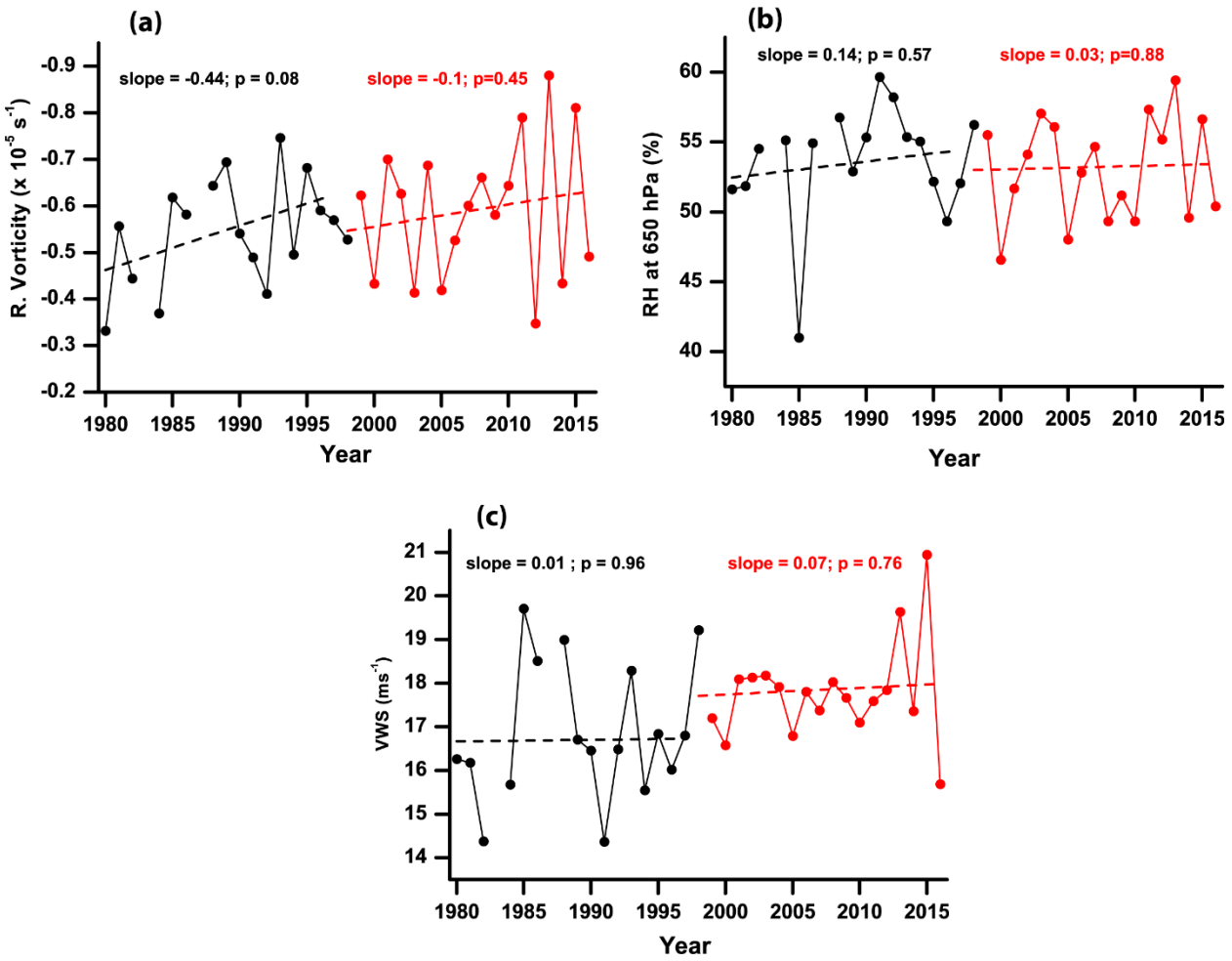

Figure 6: Time series of (a) vorticity at 850 hPa (10^{-5} s^{-1}), (b) relative humidity at 600 hPa (%), and (c) Vertical wind shear (VWS; m s^{-1}) averaged over the 1000 km from the center of the cyclone tracks. Black dotted lines indicate the trends during the 1980-1998 period, and red dashed lines indicate the trends during the 1999-2016 period. Slopes correspond to the regression value, and 'p' values are the significance of the trends.

4. Conclusion

PDI over the SIO during 1999-2016 has doubled when compared to the decades of 1980-1998 period. The motivation for splitting across 1998-1999 was based on the proposed climate

regime shift which also tends to coincide with the debate about a slowdown in global warming and changes in the frequency of the so-called Central Pacific El Niño compared to the canonical El Niño (Yeh *et al* 2009). Focusing just on the changes in the cyclone properties across the two periods, we note an increase in PDI during the latter period, which we attribute to increased cyclone intensity and duration. Analysis of the relevant atmospheric variables clearly indicates that the processes in the atmosphere did not seem to play a major role towards the cyclone intensification in the SIO. In contrast, increasing trends in SST, UOHC and a decreasing trend in cyclone translation speed during the recent decades seem to be responsible for the increase in cyclone intensity and duration and subsequently the increase in the cyclone PDI. An increase in SST and UOHC provide a more sustained supply of energy, causing a reduction in translation speed which results in the increase in cyclone duration and intensity. We show that the warming of the SIO during the 1999-2016 period is associated with a deepened thermocline, which inhibits the deeper and colder waters from cooling the surface when a cyclone passes over the region. Our findings that the ocean warming and the increase in upper ocean heat content are clearly important since the projected continuation of SIO warming can be expected to sustain the increasing trend in PDI. This will affect the most climate-vulnerable Indian Ocean island nations as well as the countries along the eastern coast of Africa. This may cause more loss of life and socioeconomic damages to the vulnerable island countries such as Mozambique (over 30 million), Mauritius (1.3 million inhabitants), and Madagascar (22 million inhabitants), which are located near the western side of the SIO. Notwithstanding the ongoing debate about the relative role of the atmospheric bridge vs. the oceanic tunnel in the low-frequency variability of this region (Deepa *et al* 2019, Jayasankar *et al* 2019a), the impact of the ocean warming on the TC genesis and their life cycle and the PDI deserve careful attention.

Acknowledgement

Authors acknowledge the Ministry of Earth Sciences, Govt. of India and Director, National Centre for Polar and Ocean Research (NCPOR), Goa for their support in this study. We sincerely thank the three anonymous reviewers for their valuable comments and suggestions which improved the quality of the manuscript significantly. RM gratefully acknowledges the Visiting Faculty position at the Indian Institute of Technology, Bombay. All the data sets used in this study are freely available, and details are mentioned in the data and method section. ORAS4 data was taken from http://apdrc.soest.hawaii.edu/las/v6/dataset?catitem=16675. ERA-interim data was taken from https://apps.ecmwf.int/datasets/data/interim-full-daily/. The NCPOR Contribution no. is XXXX and the NIO contribution no. is XXXX.

Reference:

Balmaseda M A, Mogensen K and Weaver A T 2013 Evaluation of the ECMWF ocean reanalysis system ORAS4 *Q. J. R. Meteorol. Soc.* **139** 1132–61

Bhatia K T, Vecchi G A, Knutson T R, Murakami H, Kossin J, Dixon K W and Whitlock C E 2019 Recent increases in tropical cyclone intensification rates *Nat. Commun. 10 635*

Blake E S, Landsea C W and Gibney E J 2011 *The deadliest, costliest, and most intense United States tropical cyclones from 1851 to 2010 (and other frequently requested hurricane facts),*NOAA Technical Memorandum NWS NHC-6. Miami, FL: National Oceanic and Atmospheric Administration, National Weather Service, National HurricaneCenter.

Burns J M, Subrahmanyam B, Nyadjro E S and Murty V S N 2016 Tropical cyclone activity over the Southwest Tropical Indian Ocean *J. Geophys. Res. Ocean* 121 6389- 6402.

Cane M A, Clement A C, Kaplan A, Kushnir Y, Pozdnyakov D, Seager R, Zebiak S E and Murtugudde R 1997 Twentieth-century sea surface temperature trends *Science* 275 957-960.

Dee D P, Uppala S M, Simmons A J, Berrisford P, Poli P, Kobayashi S, Andrae U, Balmaseda M A, Balsamo G, Bauer P, Bechtold P, Beljaars A C M, van de Berg L, Bidlot J, Bormann N, Delsol C, Dragani R, Fuentes M, Geer A J, Haimberger L, Healy S B, Hersbach H, Hólm E V., Isaksen L, Kållberg P, Köhler M, Matricardi M, Mcnally A P, Monge-Sanz B M, Morcrette J J, Park B K, Peubey C, de Rosnay P, Tavolato C, Thépaut J N and Vitart F 2011 The ERA-Interim reanalysis: Configuration and performance of the data assimilation system *Q. J. R. Meteorol. Soc.* **137** 553–97

Deepa J S, Gnanaseelan C, Mohapatra S, Chowdary J S, Karmakar A, Kakatkar R and Parekh A 2019 The Tropical Indian Ocean decadal sea level response to the Pacific Decadal Oscillation forcing *Clim. Dyn.* 52 5045-5058.

Dilmahamod A F, Hermes J C and Reason C J C 2016 Chlorophyll-a variability in the Seychelles-Chagos Thermocline Ridge: Analysis of a coupled biophysical model *J. Mar. Syst.* 154 220-232.

Dong L and McPhaden M J 2016 Interhemispheric SST gradient trends in the Indian ocean prior to and during the recent global warming hiatus *J. Clim.* 29 9077-9095.

Emanuel K 2000 A statistical analysis of tropical cyclone intensity *Mon. Weather Rev.* 128 1139-1152.

Emanuel K 2001 Contribution of tropical cyclones to meridional heat transport by the oceans *J. Geophys. Res. Atmos.106 14,771-14,781.*

Emanuel K 2007 Environmental factors affecting tropical cyclone power dissipation *J. Clim.* 20 5497-5509.

Emanuel K 2005 Increasing destructiveness of tropical cyclones over the past 30 years *Nature* 436 686-688.

Emanuel K, DesAutels C, Holloway C and Korty R 2004 Environmental control of tropical cyclone intensity *J. Atmos. Sci. 61 843-858.*

England M H, Mcgregor S, Spence P, Meehl G A, Timmermann A, Cai W, Gupta A Sen, Mcphaden M J, Purich A and Santoso A 2014 Recent intensification of wind-driven circulation in the Pacific and the ongoing warming hiatus. *Nature Climate Change, 4*, 222 - 227

Girishkumar M S and Ravichandran M 2012 The influences of ENSO on tropical cyclone activity in the Bay of Bengal during October-December *J. Geophys. Res. Ocean.* 117 C02033.

Hu S and Fedorov A V. 2017 The extreme El Niño of 2015–2016 and the end of global warming hiatus *Geophys. Res. Lett.* 44 31816-3824.

Hu S and Sprintall J 2017 Observed strengthening of interbasin exchange via the Indonesian seas due to rainfall intensification *Geophys. Res. Lett.* **44** 1448–56

Jayasankar T, Eldho T I, Ghosh S and Murtugudde R 2019a Assessment of the interannual variability of local atmospheric and ITF contribution to the subsurface heat content of southern tropical Indian Ocean in GECCO2 and ORAS4 using ROMS *Glob. Planet. Change 181 102974*

Jayasankar T, Murtugudde R and Eldho T I 2019b The Indian Ocean Deep Meridional Overturning Circulation in Three Ocean Reanalysis Products *Geophys. Res. Lett.* 46 084244.

Jyoti J, Swapna P, Krishnan R and Naidu C V. 2019 Pacific modulation of accelerated south Indian Ocean sea level rise during the early 21st Century *Clim. Dyn. 53 4413-4432.*

Kosaka Y and Xie S 2013a Recent global-warming hiatus tied to equatorial Pacific surface cooling *Nature* **501** 403–7 Online: http://dx.doi.org/10.1038/nature12534

Kossin J P 2018 A global slowdown of tropical-cyclone translation speed *Nature* 558 7708

Lee S K, Park W, Baringer M O, Gordon A L, Huber B and Liu Y 2015 Pacific origin of the abrupt increase in Indian Ocean heat content during the warming hiatus *Nat. Geosci.* **8** 445–9

Li T, Kwon M, Zhao M, Kug J S, Luo J J and Yu W 2010 Global warming shifts Pacific tropical cyclone location *Geophys. Res. Lett.* 37 L21804.

Lin I I, Black P, Price J F, Yang C Y, Chen S S, Lien C C, Harr P, Chi N H, Wu C C and D'Asaro E A 2013 An ocean coupling potential intensity index for tropical cyclones *Geophys. Res. Lett.*. 40 1878-1882.

Lin I I, Wu C C, Pun I F and Ko D S 2008 Upper-ocean thermal structure and the Western North Pacific category 5 typhoons. Part I: Ocean features and the category 5 typhoons' intensification *Mon. Weather Rev.* 136 3288-3306.

Liu Q Y, Feng M, Wang D and Wijffels S 2015 Interannual variability of the Indonesian Throughflow transport: A revisit based on 30 year expendable bathythermograph data *J. Geophys. Res. Ocean.* **120** 8270–82

Lyon B and Camargo S J 2009 The seasonally-varying influence of ENSO on rainfall and tropical cyclone activity in the Philippines *Clim. Dyn.* 32 125-141.

Malan N, Reason C J C and Loveday B R 2013 Variability in tropical cyclone heat potential over the Southwest Indian Ocean *J. Geophys. Res. Ocean.* 118 6734-6746.

Manatsa D, Reason C J C and Mukwada G 2012 On the decoupling of the IODZM from southern Africa Summer rainfall variability *Int. J. Climatol. 32 727-746.*

Matsuura T, Yumoto M and Iizuka S 2003 A mechanism of interdecadal variability of tropical cyclone activity over the western North Pacific *Clim. Dyn. 21 105-117.*

Mavume A, Rydberg L, Rouault M and Lutjeharms J 2010 Climatology and Landfall of Tropical Cyclones in the South- West Indian Ocean *West. Indian Ocean J. Mar. Sci. 8 15-36.*

Mawren D and Reason C J C 2017 Variability of upper-ocean characteristics and tropical cyclones in the South West Indian Ocean *J. Geophys. Res. Ocean. 122 JC012028.*

Vidya P J, Ravichandran M, Subeesh M P, Chatterjee S and Nuncio M 2020 Global warming hiatus contributed weakening of the Mascarene High in the Southern Indian Ocean *Sci. Rep.* **10** 16–9 Online: http://dx.doi.org/10.1038/s41598-020-59964-7

Rayner N A, Parker D E, Horton E B, Folland C K, Alexander L V., Rowell D P, Kent E C and Kaplan A 2003 Global analyses of sea surface temperature, sea ice, and night marine air temperature since the late nineteenth century *J. Geophys. Res. Atmos. 108 4407.*

Seager R, Cane M, Henderson N, Lee D E, Abernathey R and Zhang H 2019 Strengthening tropical Pacific zonal sea surface temperature gradient consistent with rising greenhouse gases *Nat. Clim. Chang. 9 517-522.*

Ueda H, Kamae Y, Hayasaki M, Kitoh A and Watanabe S 2015 Combined effects of recent Pacific cooling and *Nat. Commun.* **6** 1–8 Online: http://dx.doi.org/10.1038/ncomms9854

Uotila P, Vihma T, Pezza A B, Simmonds I, Keay K and Lynch A H 2011 Relationships between Antarctic cyclones and surface conditions as derived from high-resolution numerical weather prediction data *J. Geophys. Res. Atmos. 116 D07109.*

Wanson K L and Tsonis A A 2009 Has the climate recently shifted? *Geophys. Res. Lett. 36 L06711.*

Webster P J 2005 Changes in Tropical Cyclone Number, Duration, and Intensity in a Warming Environment Science 309 1844-1846.

Wing A A, Sobel A H and Camargo S J 2007 Relationship between the potential and actual intensities of tropical cyclones on interannual time scales *Geophys. Res. Lett. 34 L08810.*

Yeh S W, Kug J S, Dewitte B, Kwon M H, Kirtman B P and Jin F F 2009 El Nĩo in a changing climate *Nature 461 511-514.*

Zhang C, Li S, Luo F and Huang Z 2019a The global warming hiatus has faded away: An analysis of 2014–2016 global surface air temperatures *Int. J. Climatol. 39 4853-4868.*

Zhang L, Han W, Karnauskas K B, Meehl G A, Hu A, Rosenbloom N and Shinoda T 2019b Indian Ocean Warming Trend Reduces Pacific Warming Response to Anthropogenic Greenhouse Gases: An Interbasin Thermostat Mechanism *Geophys. Res. Lett. 46 084088.*

Zhang Y, Feng M, Du Y, Phillips H E, Bindoff N L and McPhaden M J 2018 Strengthened Indonesian Throughflow Drives Decadal Warming in the Southern Indian Ocean *Geophys. Res. Lett.* **45** 6167–75

Table 1. Represents the means of all variables during 1980-1998 and 1999-2016, and corresponding P values and T values. The values, which are significant above 95% CL, is given in red font.

Variables	**1980-1998**	**1999-2016**	**P value**	**T value**
SST (ºC)	27.72	27.86	0.14	-1.5
PDI (x10 ^{12} m^3s^{-3})	0.28	0.65	0.00	-4.58
Number	4.11	4.61	0.44	-0.78
Intensity (ms^{-1})	51.29	55.27	0.00	-3.59
Duration (days)	6.008	9.88	0.00	-4.25
VWS (ms^{-1})	16.84	17.77	0.05	-2.02
R.H. (%)	53.64	53.04	0.65	0.46
Vorticity (x 10^{-5} s^{-1})	-0.54	-0.59	0.22	1.25
UOHC (x 10^{10} Jm^{-2})	7.47	7.52	0.03	-2.24

Supplementary Figures

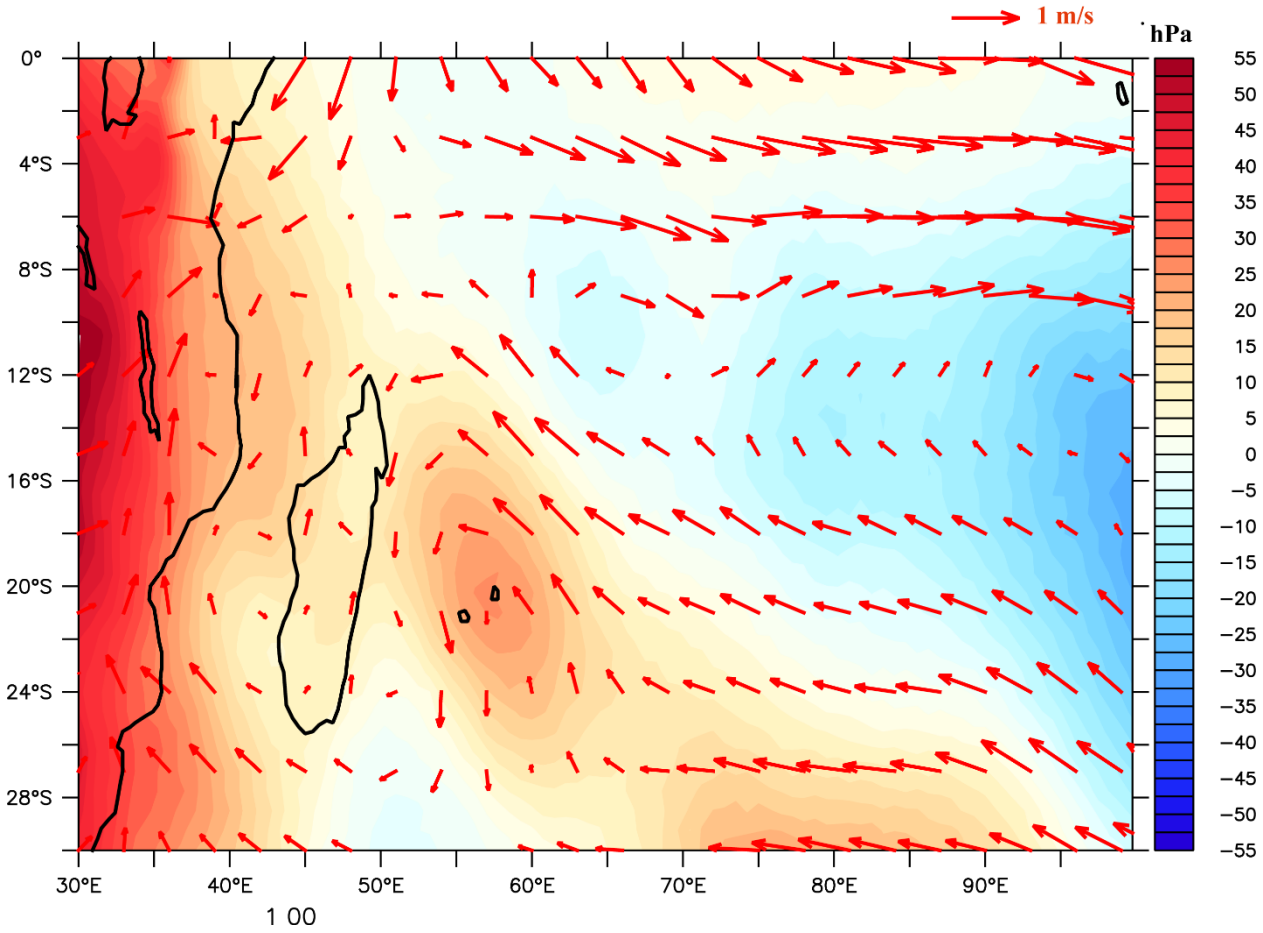

Figure S1: 850hPa Geopotential Height (m) difference (1999-2016 minus 1980-1998) overlaid with the difference in wind vectors (850 hPa).

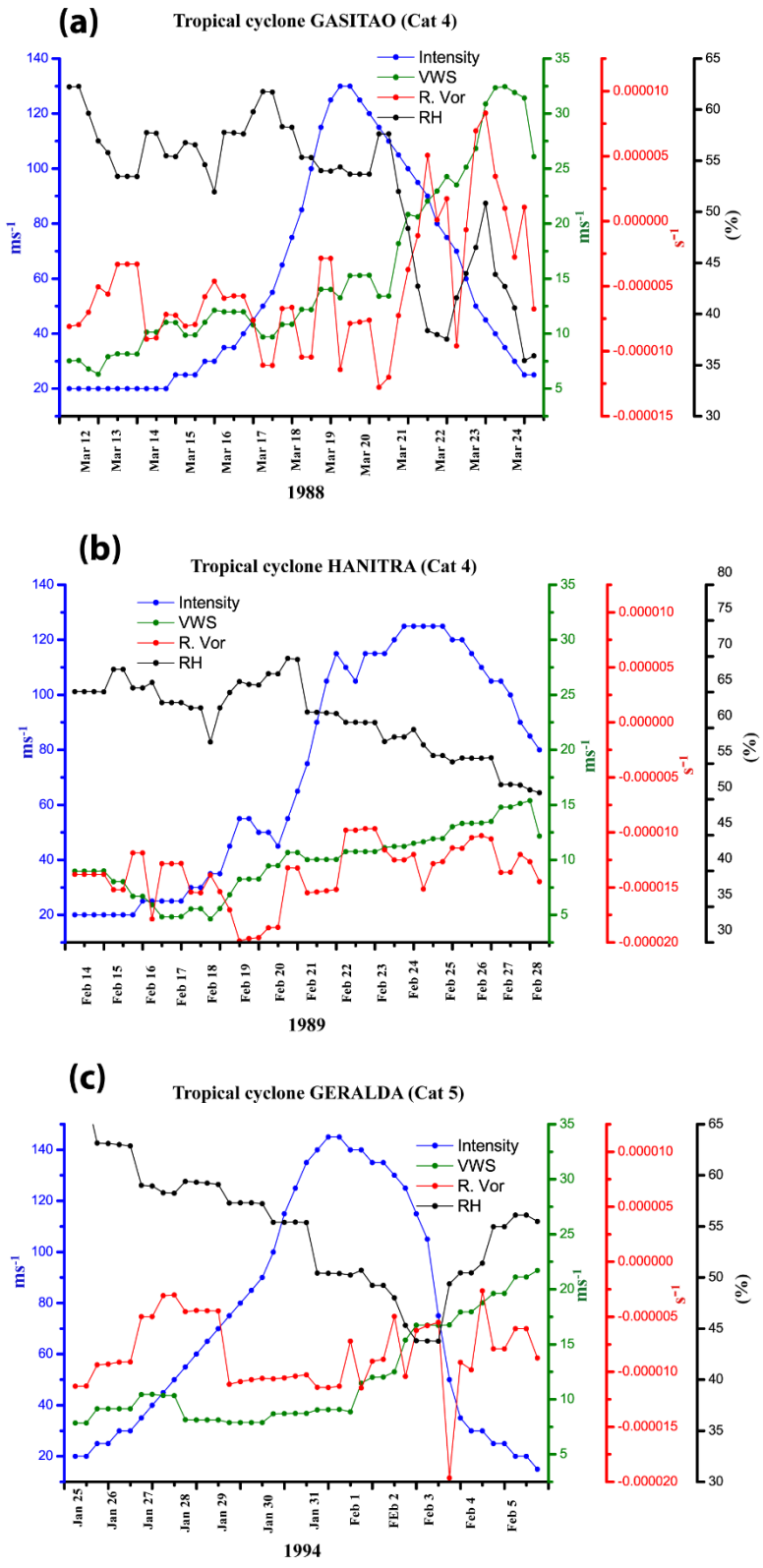

Figure S2: Variations in atmospheric parameters along the cyclone track during 1980-1998.

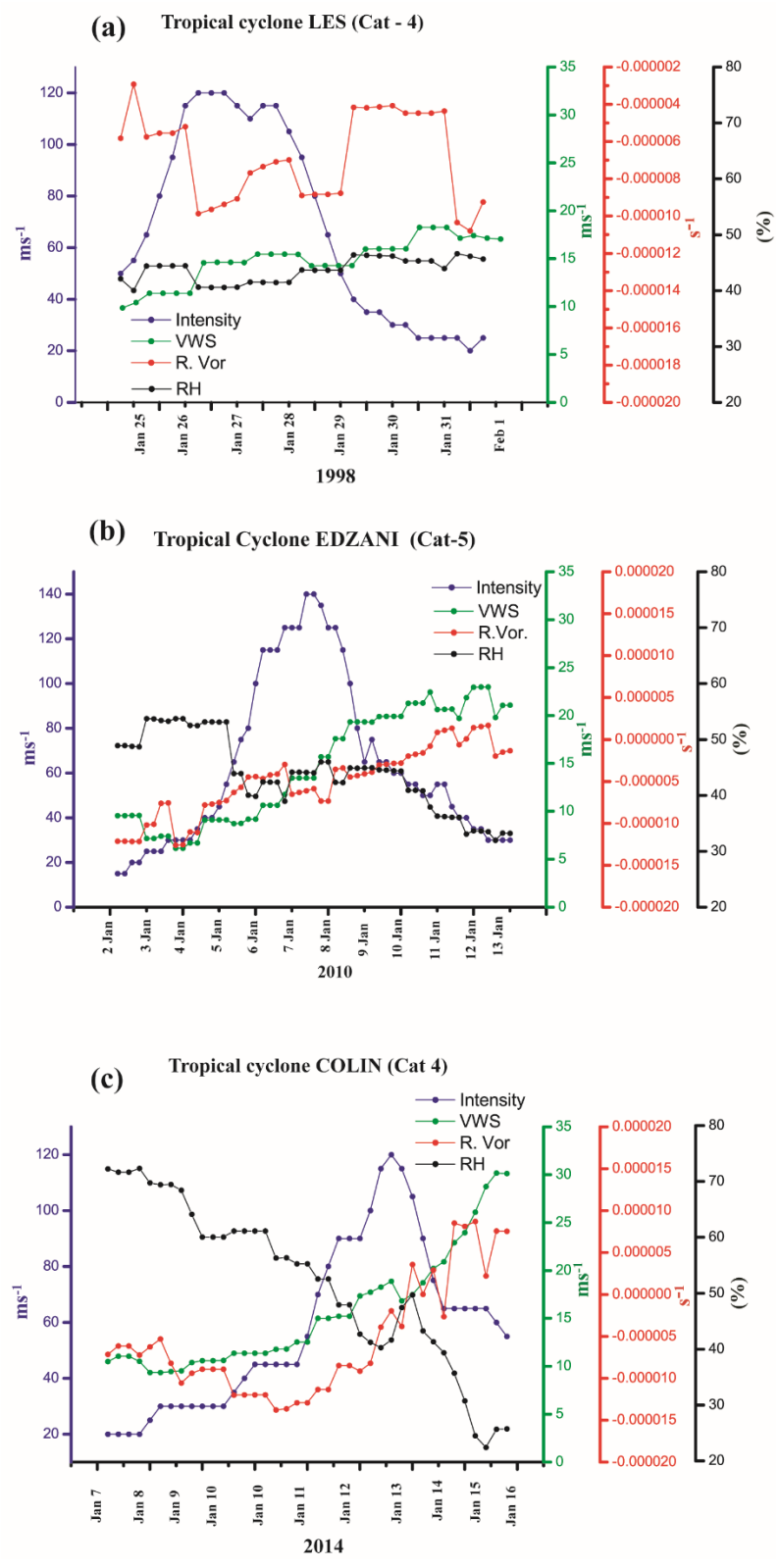

Figure S3: Variations in atmospheric parameters along the cyclone track during 1999-2016.